

## Experimental study of $pp\eta$ dynamics in the $pp \rightarrow pp\eta$ reaction

P. Moskal,<sup>1,2</sup> H.-H. Adam,<sup>3</sup> A. Budzanowski,<sup>4</sup> R. Czyżykiewicz,<sup>2</sup> D. Grzonka,<sup>1</sup> M. Janusz,<sup>2</sup> L. Jarczyk,<sup>2</sup> B. Kamys,<sup>2</sup> A. Khoukaz,<sup>3</sup> K. Kilian,<sup>1</sup> P. Kowina,<sup>1,5</sup> K. Nakayama,<sup>6</sup> W. Oelert,<sup>1</sup> C. Piskor-Ignatowicz,<sup>2</sup> J. Przerwa,<sup>2</sup> T. Rożek,<sup>1,5</sup> R. Santo,<sup>3</sup> G. Schepers,<sup>1</sup> T. Sefzick,<sup>1</sup> M. Siemaszko,<sup>5</sup> J. Smyrski,<sup>2</sup> S. Steltenkamp,<sup>3</sup> A. Täschner,<sup>3</sup> P. Winter,<sup>1</sup> M. Wolke,<sup>1</sup> P. Wüstner,<sup>7</sup> and W. Zipper<sup>5</sup>

<sup>1</sup>*Institut für Kernphysik, Forschungszentrum Jülich, D-52425 Jülich, Germany*

<sup>2</sup>*Institute of Physics, Jagellonian University, PL-30-059 Cracow, Poland*

<sup>3</sup>*Institut für Kernphysik, Westfälische Wilhelms-Universität, D-48149 Münster, Germany*

<sup>4</sup>*Institute of Nuclear Physics, PL-31-342 Cracow, Poland*

<sup>5</sup>*Institute of Physics, University of Silesia, PL-40-007 Katowice, Poland*

<sup>6</sup>*Department of Physics and Astronomy, University of Georgia, Athens, Georgia 30602, USA*

<sup>7</sup>*Zentrallabor für Elektronik, Forschungszentrum Jülich, D-52425 Jülich, Germany*

(Received 4 July 2003; revised manuscript received 3 September 2003; published 19 February 2004)

A high statistics measurement of the  $pp \rightarrow pp\eta$  reaction at an excess energy of  $Q=15.5$  MeV has been performed at the internal beam facility COSY-11. The stochastically cooled proton beam and the used detection system allowed to determine the momenta of the outgoing protons with a precision of  $4 \text{ MeV}/c$  ( $\sigma$ ) in the center-of-mass frame. The determination of the four-momentum vectors of both outgoing protons allowed to derive the complete kinematical information of the  $\eta pp$  system. An unexpectedly large enhancement of the occupation density in the kinematical regions of low proton- $\eta$  relative momenta is observed. A description taking the proton-proton and the  $\eta$ -proton interaction into account and assuming an on-shell incoherent pair-wise interaction among the produced particles fails to explain this strong effect. Its understanding will require a rigorous three-body approach to the  $pp\eta$  system and the precise determination of contributions from higher partial waves. We also present an invariant mass spectrum of the proton-proton system determined at  $Q=4.5$  MeV. Interestingly, the enhancement at large relative momenta between protons is visible also at such a small excess energy. In contrast to all other determined angular distributions, the orientation of the emission plane with respect to the beam direction is extracted to be anisotropic.

DOI: 10.1103/PhysRevC.69.025203

PACS number(s): 13.60.Le, 13.75.-n, 13.85.Lg, 25.40.-h

### I. MANIFESTATION OF THE $\eta pp$ INTERACTION

Due to the short life time of the flavor-neutral mesons (e.g.,  $\pi^0$ ,  $\eta$ ,  $\eta'$ ), the study of their interaction with nucleons or with other mesons is at present not feasible in direct scattering experiments. One of the methods permitting such investigations is the production of a meson in the nucleon-nucleon interaction close to the kinematical threshold or in kinematics regions where the outgoing particles possess small relative velocities. A mutual interaction among the outgoing particles manifests itself in the distributions of differential cross sections as well as in the magnitude and energy dependence of the total reaction rate.

In the last decade major experimental [1–8] and theoretical [9–13] efforts were concentrated on the study of the creation of  $\pi^0$ ,  $\eta$ , and  $\eta'$  mesons via the hadronic interactions [14–16]. Measurements have been made in the vicinity of the kinematical threshold where only a few partial waves in both initial and final states are expected to contribute to the production process. This simplifies significantly the interpretation of the data, yet it appears to be challenging due to the three-particle final state system with a complex hadronic potential.

The determined energy dependences of the total cross section for  $\eta'$  [1,2] and  $\eta$  [2–6] mesons in proton-proton collisions are presented in Fig. 1. Comparing the data to the arbitrarily normalized phase-space integral (dashed lines) reveals that the proton-proton FSI enhances the total cross sec-

tion by more than an order of magnitude for low excess energies. One recognizes also that in the case of the  $\eta'$  the data are described very well (solid line) assuming that the on-shell proton-proton amplitude exclusively determines the phase-space population. This indicates that the proton- $\eta'$  interaction is too small to manifest itself in the excitation function within the presently achievable accuracy. In case of the  $\eta$  meson the increase of the total cross section for very low and very high energies is much larger than expected from the  $^1S_0$  final state interaction between protons (solid line), though for both the  $pp \rightarrow pp\eta$  and  $pp \rightarrow pp\eta'$  reactions the dominance of the  $^3P_0 \rightarrow ^1S_0 s$  transition<sup>1</sup> is expected up to an excess energy of about 40 MeV and 100 MeV, respectively [14]. The excess at higher energies can be assigned to the

<sup>1</sup>The transition between angular momentum combinations of the initial and final states are described according to the conventional notation [8] in the following way:

$$2^{S_i+1}L_{J_i}^i \rightarrow 2^{S_f+1}L_{J_f}^f, \quad (1)$$

where superscript  $i$  indicates the initial state quantities.  $S$  denotes the spin of the nucleons, and  $J$  stands for their overall angular momentum.  $L$  and  $l$  denote the relative angular momentum of the nucleon-nucleon pair and of the meson relative to the  $NN$  system, respectively. The values of orbital angular momenta are commonly expressed using the spectroscopic notation ( $L=S, P, D, \dots$ , and  $l=s, p, d, \dots$ ).

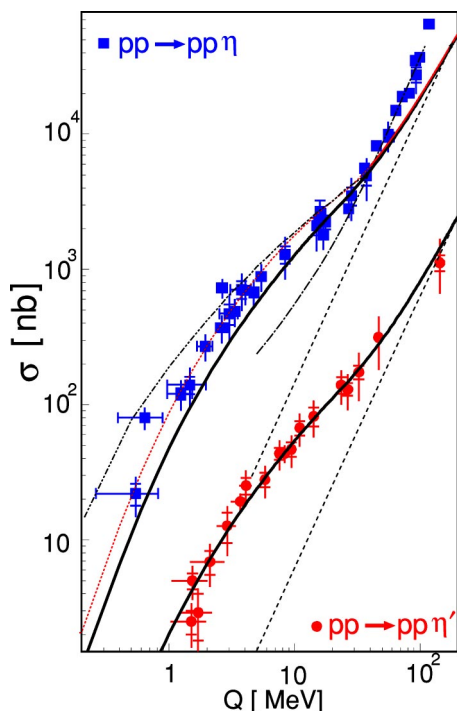


FIG. 1. Total cross section for the reactions  $pp \rightarrow pp\eta'$  (circles) and  $pp \rightarrow pp\eta$  (squares) as a function of the center-of-mass excess energy  $Q$ . Data are from Refs. [1–6]. The dashed lines indicate a phase-space integral normalized arbitrarily. The solid lines show the phase-space distribution with inclusion of the  $^1S_0$  proton-proton strong and Coulomb interactions. In case of the  $pp \rightarrow pp\eta$  reaction the solid line was fitted to the data in the excess energy range between 15 and 40 MeV. Additional inclusion of the proton- $\eta$  interaction is indicated by the dotted line. The scattering length of  $a_{p\eta} = 0.7 \text{ fm} + i 0.4 \text{ fm}$  and the effective range parameter  $r_{p\eta} = -1.50 \text{ fm} - i 0.24 \text{ fm}$  [17] have been arbitrarily chosen. The dash-dotted line represents the energy dependence taking into account the contribution from the  $^3P_0 \rightarrow ^1S_0s$ ,  $^1S_0 \rightarrow ^3P_0s$ , and  $^1D_2 \rightarrow ^3P_2s$  transitions [11]. Preliminary results for the  $^3P_0 \rightarrow ^1S_0s$  transition with the full treatment of the three-body effects are shown as a dashed-double-dotted line [18]. The absolute scale of dashed-double-dotted line was arbitrarily fitted to demonstrate the energy dependence only.

significant onset of higher partial waves, and the influence of the attractive interaction between the  $\eta$  meson and the proton could be a plausible explanation for the enhancement at threshold. A similar effect close to threshold is also observed in the photoproduction of  $\eta$  via the  $\gamma d \rightarrow pn\eta$  reaction [19] indicating to some extent that the phenomenon is independent of the production process but rather related to the interaction among the  $\eta$  meson and nucleons in the  $S_{11}(1535)$  resonance region. Indeed, a simple phenomenological treatment [13,14,20]—based on factorization of the transition amplitude into the constant primary production and the on-shell incoherent pairwise interaction among outgoing particles—describes very well the enhancement close to the threshold (dotted line). However, this approach fails for the description of the invariant mass distribution of the proton-proton and proton- $\eta$  subsystems determined recently at  $Q = 15 \text{ MeV}$  by the COSY-TOF Collaboration [21]. The struc-

ture of this invariant mass distribution, which we confirm in this paper utilizing a fully different experimental method, may indicate a non-negligible contribution from the  $P$  waves in the outgoing proton-proton subsystem [11]. These can be produced for instance via  $^1S_0 \rightarrow ^3P_0s$  or  $^1D_2 \rightarrow ^3P_2s$  transitions. This hypothesis encounters, however, difficulties in describing the excess energy dependence of the total cross section. The amount of the  $P$ -wave admixture derived from the proton-proton invariant mass distribution leads to a good description of the excitation function at higher excess energies, while at the same time it spoils significantly the agreement with the data at low values of  $Q$ , as depicted by the dash-dotted line in Fig. 1. However, these difficulties in reproducing the observed energy dependence might be due to the particular model used in Ref. [11], and thus higher partial wave contributions cannot *a priori* be excluded. In contrast to the  $P$ -wave contribution the three-body treatment [18] of the  $pp\eta$  system (dashed-double-dotted line) leads to an even larger enhancement of the cross section near threshold than that based on the Ansatz of the factorization of the proton-proton and proton- $\eta$  interactions. It must be kept in mind however that a too strong FSI effect predicted by the three-body model must be partially assigned to the neglect of the Coulomb repulsion in these preliminary calculations [18]. These illustrate that the simple phenomenological approach shown by the dotted line could fortuitously lead to the proper result, due to a mutual cancellation of the effects caused by the approximations assumed in calculations and the neglect of higher partial waves. This issue will be discussed further in Sec. IV after the presentation of the new COSY-11 data. The above considerations show unambiguously that for the complete understanding of the low-energy  $pp\eta$  dynamics, in addition to the already established excitation function of the total cross section, a determination of the differential observables is also necessary.

These will help to disentangle effects caused by the proton- $\eta$  interaction and the contributions from higher partial waves. In this paper we present differential distributions determined experimentally for variables fully describing the  $pp\eta$  system produced at an excess energy of  $Q = 15.5 \text{ MeV}$  via the  $pp \rightarrow pp\eta$  reaction.

## II. CHOICE OF OBSERVABLES

For the full description of the three-particle system five independent variables are required. In the center-of-mass frame, due to the momentum conservation, the momentum vectors of the particles are lying in one plane often referred to as the emission, reaction, or decay plane. In this plane (depicted in Fig. 2) a relative movement of the particles can be described by two variables only. The square of the invariant masses of the di-proton and proton- $\eta$  system denoted as  $s_{pp}$  and  $s_{p\eta}$  respectively, constitute a natural choice for the study of the interaction within the  $pp\eta$  system. This is because in the case of noninteracting objects the surface spanned by these variables is homogeneously populated. The interaction among the particles modifies that occupation density and in consequence facilitates an easy qualitative interpretation of the experimental results.

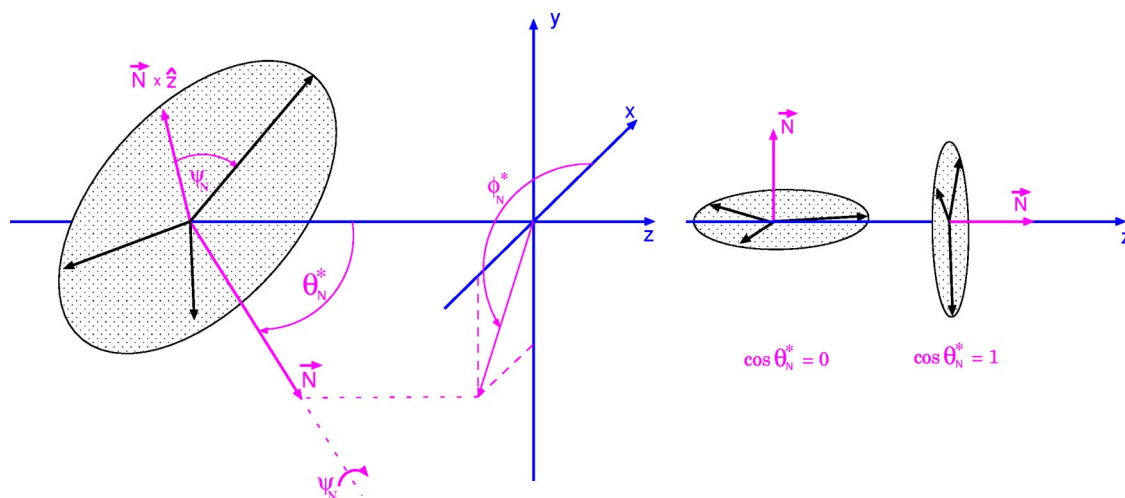


FIG. 2. Definition of the center-of-mass kinematical variables used in this article for the description of the  $pp\eta$  system.  $\vec{N}$  is a vector normal to the emission plane, which can be calculated as the vector product of the center-of-mass momentum vectors of the outgoing protons. As an example two extreme orientations of the emission plane are shown in the right panel. For further description see the text.

The remaining three variables must define an absolute orientation of the emission plane in the distinguished coordinate system. Following Ref. [22] we will use the azimuthal and polar angle of the vector normal to that plane. These angles are shown in Fig. 2 as  $\phi_N^*$  and  $\theta_N^*$ , respectively. Further the absolute orientation of the particles momenta in the emission plane will be described by  $\psi_N$ , the angle between  $\eta$  meson and the vector product of the beam momentum and the vector  $\vec{N}$ .

Obviously, the interaction between the particles does not depend on the orientation of the emission plane, and therefore, it will fully manifest itself in the occupation density of the Dalitz plot which in our case will be represented in terms of the square of the invariant masses of the two-particle subsystems. The distribution of the orientation of the emission plane will reflect, however, the correlation between the initial and final channels and hence its determination should be helpful for the investigation of the production mechanism.

### III. EXPERIMENT AND DATA ANALYSIS

Using the COSY-11 detection system [23,24], utilizing a stochastically cooled proton beam of the cooler synchrotron COSY [25] and a hydrogen cluster target [26], we have performed a high statistics measurement of the  $pp \rightarrow pp\eta$  reaction at a nominal beam momentum of 2.027 GeV/c.

The experiment was based on the four-momentum registration of both outgoing protons, whereas the  $\eta$  meson was identified via the missing mass technique. The positively charged particles have been identified combining the time of flight between the S1 and S3 scintillation detectors and the momentum reconstructed by tracking trajectories registered by means of the drift chambers back to the target. The detection setup is sketched in Fig. 3.

After the selection of events with two registered protons, the data were corrected for the mean beam momentum changes determined from the measured Schottky frequency spectra and the known beam optics. Furthermore, from the

distributions of the elastically scattered protons, the Schottky frequency spectrum, and the missing mass distribution of the  $pp \rightarrow ppX$  reaction, we have estimated that the spread of the beam momentum, and the spread of the reaction points in horizontal and vertical direction amounted to  $\sigma(p_{beam}) = 0.63 \pm 0.03$  MeV/c,  $\sigma(x) = 0.22 \pm 0.02$  cm, and  $\sigma(y)$

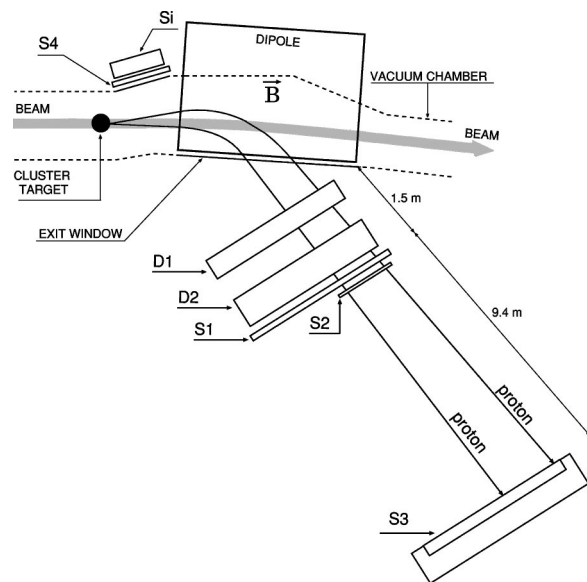


FIG. 3. Schematic view of the COSY-11 detection setup [23]. The cluster target [26] is located in front of the accelerator dipole magnet. Positively charged particles which leave the scattering chamber through the thin exit foil are detected in two drift chamber stacks D1, D2 and in the scintillator hodoscopes S1, S2, and S3. Scintillation detector S4 and the position sensitive silicon pad detector Si are used in coincidence with the S1 counter for the registration of the elastically scattered protons. Elastic scattering is used for an absolute normalization of the cross sections of the investigated reactions and for monitoring both the geometrical spread of the proton beam and the position at which beam crosses the target [24].

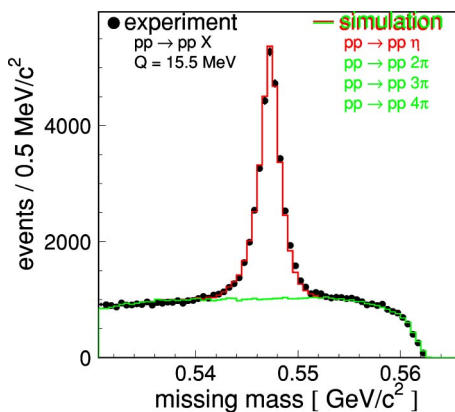


FIG. 4. Missing mass spectrum for the  $pp \rightarrow ppX$  reaction determined in the experiment at a beam momentum of 2.0259 GeV/c. The mass resolution amounts to 1 MeV/c<sup>2</sup>( $\sigma$ ). The superimposed histograms present the simulation for  $1.5 \times 10^8$  events of the  $pp \rightarrow pp\eta$  reaction, and  $10^{10}$  events for the reactions  $pp \rightarrow pp2\pi$ ,  $pp \rightarrow pp3\pi$ , and  $pp \rightarrow pp4\pi$ . The simulated histograms were fitted to the data varying only the magnitude. The fit resulted in  $24009 \pm 210$  events with the production of the  $\eta$  meson.

$=0.38 \pm 0.04$  cm, respectively. Details of this procedure can be found in Refs. [24,27].

A missing mass spectrum determined after correction for effects of the time dependent relative shifts between the beam and the target is shown in Fig. 4.

The peak originating from the  $pp \rightarrow pp\eta$  reaction is clearly recognizable over the background of multipion production. As can be observed in Fig. 4 the simulation describes the data very well. The calculated spectrum is hardly distinguishable from the experimental points. The background was estimated taking into account  $pp \rightarrow ppX$  reactions with  $X=2\pi, 3\pi$ , and  $4\pi$ .

The position of the peak on the missing mass spectrum and the known mass of the  $\eta$  meson [28] enabled to determine the actual absolute beam momentum to be  $p_{beam} = 2.0259$  GeV/c  $\pm$  0.0013 GeV/c, which agrees within error limits with the nominal value of  $p_{beam}^{nominal} = 2.0270$  GeV/c. The real beam momentum corresponds to the excess energy of the  $pp\eta$  system equal to  $Q = 15.5 \pm 0.4$  MeV.

#### A. Covariance matrix and kinematical fitting

As already mentioned in the preceding section at the COSY-11 facility the identification of the  $pp \rightarrow pp\eta$  reaction is based on the measurement of the momentum vectors of the outgoing protons and the utilization of the missing mass technique. Inaccuracy of the momentum determination manifests itself in the population of kinematically forbidden regions of the phase space, preventing a precise comparison of the theoretically derived and experimentally determined differential cross sections. Figure 5 visualizes this effect and clearly demonstrates that the data scatter significantly outside the kinematically allowed region (solid line).

Therefore, when seeking for small effects like, for example, the influence of the proton- $\eta$  interaction on the popu-

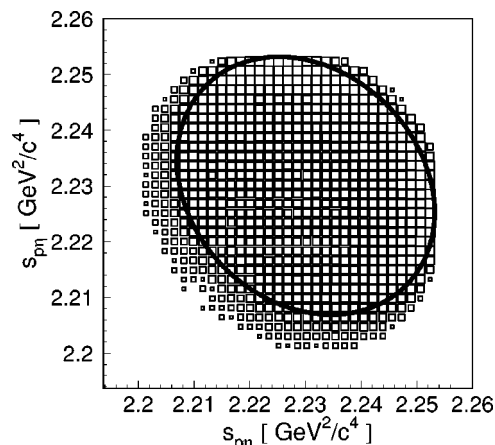


FIG. 5. Dalitz plot distribution of the  $pp \rightarrow pp\eta$  reaction simulated at  $Q=15.5$  MeV. The number of entries is shown in a logarithmic scale. The solid line gives the kinematically allowed area. The result was obtained taking into account the experimental conditions as described in the text.

lation density of the phase space, one needs either to fold theoretical calculations with the experimental resolution or to perform the kinematical fitting of the data. Both procedures require the knowledge of the covariance matrix, and thus its determination constitutes a necessary step in the differential analysis and interpretation of the data.

In order to derive the covariance matrix we need to recognize and quantify all possible sources of errors in the reconstruction of the two proton momenta  $\vec{p}_1$  and  $\vec{p}_2$ . The four dominant effects are (i) finite distributions of the beam momentum and of the reaction points, (ii) multiple scattering in the dipole chamber exit foil, air, and detectors, (iii) finite resolution of the position determination of the drift chambers, and (iv) a possible inadequate assignment of hits to the particle tracks in drift chambers in the case of very close tracks.

In order to estimate the variances and covariances for all possible combinations of the momentum components of two registered protons we have generated  $1.5 \times 10^8$   $pp \rightarrow pp\eta$  events and simulated the response of the COSY-11 detection setup taking into account the above listed factors and the known resolutions of the detector components. Next, we analyzed the signals by means of the same reconstruction procedure as used in case of the experimental data.

Since inaccuracies of the momentum determination depend on the particle momentum itself (e.g., multiple scattering) and on the relative momentum between protons (e.g., trajectories reconstruction from signals in drift chambers), we have determined the covariance matrices as a function of the absolute momentum of both protons. In the experiment we have measured six variables and once we assume that the event corresponds to the  $pp \rightarrow pp\eta$  reaction only five of them are independent. Thus we have varied the values of the event components demanding that the missing mass is equal to the mass of the  $\eta$  meson and we have chosen that vector which was the closest to the experimental one. The inverse of the

covariance matrix was used as a metric for the distance calculation. The kinematical fit improves the resolution by a factor of about 1.5. The finally resulting error of the momentum determination amounts to 4 MeV/c.

### B. Multidimensional acceptance corrections and results

At the excess energy of  $Q=15.5$  MeV the COSY-11 detection system does not cover the full  $4\pi$  solid angle in the center-of-mass system of the  $pp \rightarrow pp\eta$  reaction. Therefore, the detailed study of differential cross sections requires corrections for the acceptance. Generally, the acceptance should be expressed as a function of the full set of mutually orthogonal variables which describe the studied reaction unambiguously. To define the relative movement of the particles in the reaction plane we have chosen two squares of the invariant masses:  $s_{pp}$  and  $s_{p\eta}$  and to define the orientation of this plane in the center-of-mass frame we have taken the three Euler angles: The first two are simply the polar  $\phi_\eta^*$  and azimuthal  $\theta_\eta^*$  angles of the momentum of the  $\eta$  meson and the third angle  $\psi$  describes the rotation of the reaction plane around the axis defined by the momentum vector of the  $\eta$  meson. In the data evaluation we considerably benefit from the basic geometrical symmetries satisfied by the  $pp \rightarrow pp\eta$  reaction. Due to the axial symmetry of the initial channel of the two unpolarized colliding protons the event distribution over  $\phi_\eta^*$  must be isotropic. Thus, we can safely integrate over  $\phi_\eta^*$  ignoring that variable in the analysis. Furthermore, taking advantage of the symmetry due to the two identical particles in the initial channel, without losing the generality, we can express the acceptance as a function of  $s_{pp}, s_{p\eta}, |\cos(\theta_\eta^*)|$  and  $\psi$ . To facilitate the calculations we have divided the range of  $|\cos(\theta_\eta^*)|$  and  $\psi$  into ten bins and both  $s_{pp}$  and  $s_{p\eta}$  into 40 bins each. In the case of the  $s_{pp}$  and  $s_{p\eta}$  the choice was made such that the width of the interval corresponds to the standard deviation of the experimental accuracy. For  $|\cos(\theta_\eta^*)|$  and  $\psi$  we have taken only ten partitions since from the previous experiments we expect only a small variation of the cross section over these variables [21,29,30]. In this representation, however, the COSY-11 detection system covers only 50% of the phase space for the  $pp \rightarrow pp\eta$  reaction at  $Q=15.5$  MeV. To proceed with the analysis we assumed that the distribution over the angle  $\psi$  is isotropic as it was, for example, experimentally determined for the  $pp \rightarrow pp\omega$ ,  $pp \rightarrow pp\rho$ , or  $pp \rightarrow pp\phi$  reactions [29,31]. Please note that this is the only assumption of the reaction dynamics performed in the present evaluation. The validity of this supposition in the case of the  $pp \rightarrow pp\eta$  reaction will be discussed later.

The distribution of the polar angle of the  $\eta$  meson as derived from the data after the acceptance correction was found to be isotropic within the statistical accuracy. Taking into account this angular distribution of the cross section we can calculate the acceptance as a function of  $s_{pp}$  and  $s_{p\eta}$  only. This is shown in Fig. 6, where one sees that now the full phase space is covered. This allows us to determine the distributions of  $s_{pp}$  and  $s_{p\eta}$ .

Knowing the distribution of the polar angle of the  $\eta$  meson  $\theta_\eta^*$  and those for the invariant masses  $s_{pp}$  and  $s_{p\eta}$  we can check whether the assumption of the isotropy of the cross

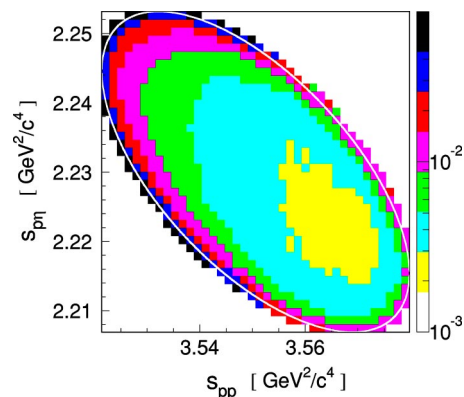


FIG. 6. COSY-11 detection acceptance as a function of  $s_{pp}$  and  $s_{p\eta}$  calculated under the assumption that the differential cross sections  $d\sigma/d\cos(\theta_\eta^*)$  and  $d\sigma/d\psi$  are isotropic.

section distribution versus the third Euler's angle  $\psi$  is corroborated by the data. For that purpose we calculated the acceptance as a function of  $\psi$  and  $s_{p\eta}$  assuming the shape of the differential cross sections of  $d\sigma/ds_{pp}$  and  $d\sigma/d\cos(\theta_\eta^*)$  as determined experimentally. Unexpectedly, contrary to the assumption made at the beginning, the cross section distribution in  $d\sigma/d\psi$  was found to be anisotropic. Therefore we performed a full acceptance correction procedure from the very beginning assuming that the distribution of  $d\sigma/d\psi$  is as determined from the data. After repeating the procedure three times we observed that the input and resultant distributions are in good agreement. The result after the third iteration is shown in Fig. 7 by the full circles. To raise the confidence in

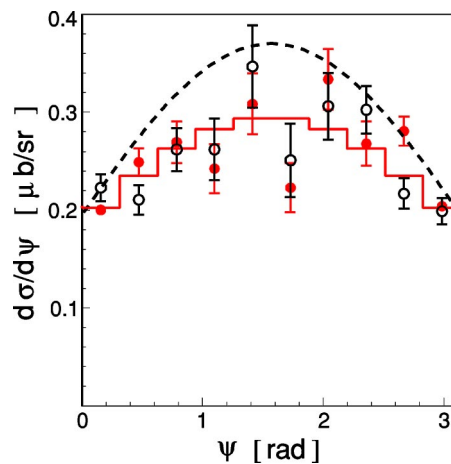


FIG. 7. Distribution of the cross section as a function of the angle  $\psi$ . Full circles stand for the final results of the  $d\sigma/d\psi$  obtained after three iterations. The superimposed histogram (solid line) corresponds to the fit of the function  $d\sigma/d\psi = a + b|\sin(\psi)|$  which resulted in  $a = 0.186 \pm 0.004 \mu\text{b/sr}$  and  $b = 0.110 \pm 0.014 \mu\text{b/sr}$ . The dashed line shows the entry distribution used for the second series of iterations as described in the text. Open circles represent the data from the left upper corner of the Dalitz plot (see, for example, Fig. 6). At that region of the Dalitz plot due to the nonzero four-dimensional acceptance over  $[s_{pp}, s_{p\eta}, |\cos(\theta_\eta^*)|, \psi]$  bins the spectrum (open circles) was corrected without a necessity of any assumptions concerning the reaction cross section.

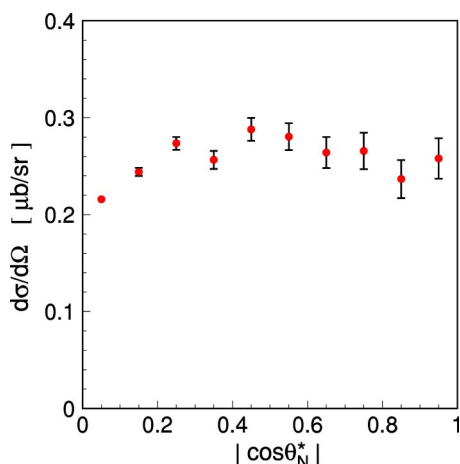


FIG. 8. Differential cross section as a function of the polar angle of the vector normal to the emission plane.

the convergence of the performed iteration we accomplished the full procedure once more, but now assuming that the distribution of  $d\sigma/d\psi$  is much more anisotropic than determined from the data. As an entry distribution we took the dashed line shown in Fig. 7. Again after two iterations we got the same result as before. To corroborate this observation we have evaluated the distribution over  $\psi$  angle (see Fig. 7) from the phase-space region which has no holes in the acceptance expressed as a four-dimensional function of the variables  $s_{pp}, s_{p\eta}, |\cos(\theta_\eta^*)|$ , and  $\psi$ , this is for the values of  $s_{pp}$  and  $s_{p\eta}$  corresponding to the upper left corner of Fig. 6. Again the obtained distribution presented as open circles in Fig. 7 is anisotropic, and moreover agrees with the spectrum determined from all events. The deviation from isotropy cannot be assigned to any unknown behavior of the background since the obtained distribution can be regarded as background free. This is because the number of  $pp \rightarrow pp\eta$  events was elaborated for each invariant mass interval separately. The comparison of the simulated distributions with the data showed that the shape of the background is well reproduced not only for the overall missing mass spectrum as shown previously in Fig. 4 but also locally in each region of the phase space. Since the experimental data are quite well described by the simulations we can rather exclude the possibility of a significant systematical error which could cause the observed anisotropy of the differential cross section  $d\sigma/d\psi$ . The anisotropy of the cross section in the  $\psi$  angle reflects itself in an anisotropy of the orientation of the emission plane.

The cross section distribution in the polar angle  $\theta_N^*$  of the vector normal to that plane is shown in Fig. 8 and the corresponding values are listed in Table I (see the electronic addendum to this paper [32]).

The distribution is not isotropic, which is particularly visible for the low values of  $|\cos(\theta_N^*)|$  burdened with small errors. As depicted in Fig. 2 the  $|\cos(\theta_N^*)|=0$  denotes such configuration of the ejectiles momenta in which the emission plane comprises the beam axis. In that case the acceptance of the COSY-11 detection system is much larger than for the

configuration where the emission plane is perpendicular to the beam. Due to this reason the error bars in Fig. 8 increase with growth of  $|\cos(\theta_N^*)|$ . It is worth stressing that the tendency of the  $pp\eta$  system to be produced, preferentially if the emission plane is perpendicular to the beam is in line with the preliminary analysis of the experiment performed by the TOF Collaboration [22]. Elucidation of that nontrivial behavior can reveal interesting features of the dynamics of the production process.

It is important to note that the shape of the  $s_{pp}, s_{p\eta}$ , and  $\cos(\theta_\eta^*)$  distributions remains unchanged during the whole iteration procedure.

### C. Total and differential cross sections

Though the form of the  $s_{pp}, s_{p\eta}$  and  $\cos(\theta_\eta^*)$  is independent of the  $\psi$  distribution, the total cross section derived from the data depends on the shape of  $d\sigma/d\psi$  quite significantly. It amounts to  $3.24 \pm 0.03 \mu\text{b}$ , yet it changes by  $\pm 0.2 \mu\text{b}$  when varying the parameters of the function  $d\sigma/d\psi = a + b|\sin(\psi)|$  by  $\pm$  three standard deviations. Therefore, we use that variation as an estimation of the systematic error in the acceptance correction. To this we must add a 3% systematical uncertainty stemming from the luminosity determination [27]. The luminosity was extracted from the comparison of the measured differential distribution of the elastically scattered protons with the results of the EDDA Collaboration [33]. The determined value amounts to  $811 \pm 8 \pm (3\%) \text{ nb}^{-1}$ . Thus the overall systematical error of the cross section value amounts to  $0.30 \mu\text{b}$ .

In summary, we determined that at  $Q=15.5 \text{ MeV}$  the total cross section for the  $pp \rightarrow pp\eta$  reaction is equal to  $3.24 \pm 0.03 \pm 0.30 \mu\text{b}$ , where the first and second errors denote the statistical and systematical uncertainty, respectively [34].

In the following we will present the values for the determined differential cross sections. If possible the data will be compared to the result of measurements performed at the nonmagnetic spectrometer COSY-TOF [21]. An interpretation of the elaborated distribution follows in the following section. The distributions of the squared invariant masses are listed in Table II of Ref. [32], and corresponding figures are shown in the following section. The distribution of the polar angle of the  $\eta$  meson emission in the center-of-mass system is given in Table I of Ref. [32] and shown in Fig. 9.

Clearly, our data agree very well with the angular dependence determined by the TOF Collaboration.

Since one of the important issues which we will discuss in the following section is the contribution from higher partial waves, we evaluated also an angular distribution of the relative momentum of two protons seen from the proton-proton center-of-mass subsystem (see Fig. 10). The distribution of that angle should deliver information about the partial waves of the proton-proton system in the exit channel.

In case of the two-body scattering, the beam direction, which is at the same time the line along which the center-of-mass system is moving, constitutes the reference frame for the angular distributions. For a three-body final state, however, the beam axis is not a good direction to look for the

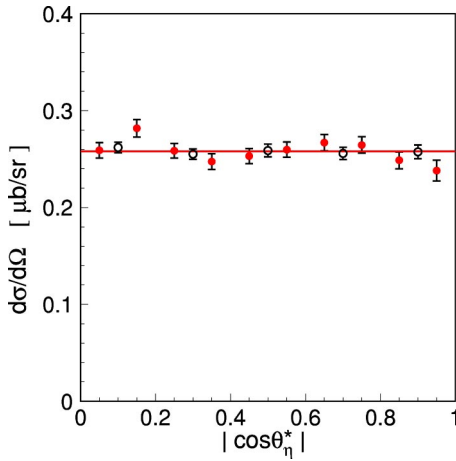


FIG. 9. Differential cross section of the  $pp \rightarrow pp\eta$  reaction as a function of the  $\eta$  meson center-of-mass polar angle. Full circles depict experimental results for the  $pp \rightarrow pp\eta$  reaction measured at  $Q=15.5$  MeV by the COSY-11 Collaboration (this article) and the open circles were determined by the TOF Collaboration at  $Q=15$  MeV [21]. The TOF points were normalized in amplitude to our result, since for that data the absolute scale is not evaluated.

angular distributions relevant for the relative angular momenta of the two particles [35]. But by analogy to the two-body system, an instructive reference axis for angular distributions in the proton-proton subsystem is now the momentum of the recoil  $\eta$  meson, since the direction of that

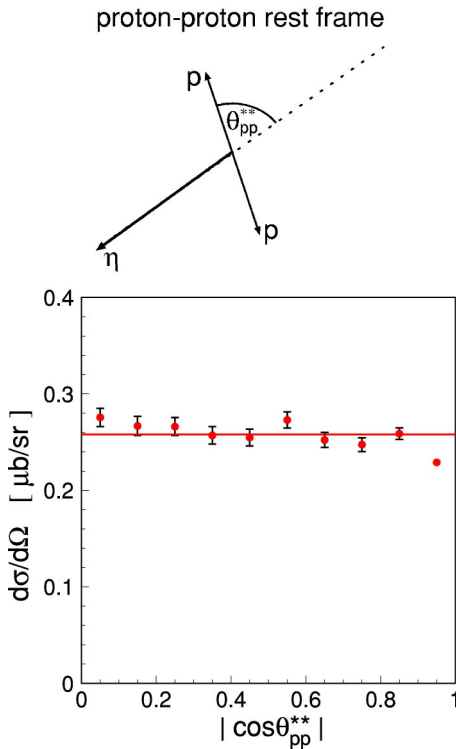


FIG. 10. Definition of  $\theta_{pp}^{**}$ , the polar angle of the relative proton-proton momentum with respect to the momentum of the  $\eta$  meson as seen in the di-proton rest frame. Lower picture shows differential cross section in  $\theta_{pp}^{**}$  as determined for the  $pp \rightarrow pp\eta$  reaction at  $Q=15.5$  MeV.

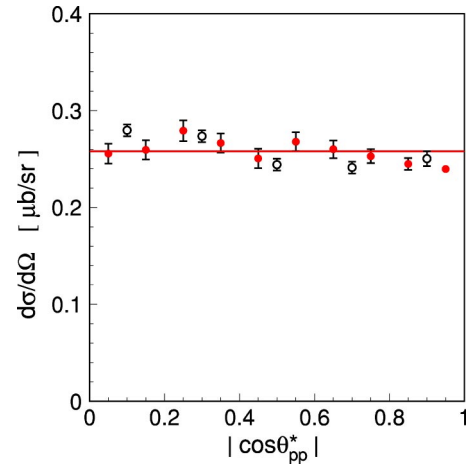


FIG. 11. Distribution of the center-of-mass polar angle of the relative protons momentum with respect to the beam direction determined for the  $pp \rightarrow pp\eta$  reaction at  $Q=15.5$  MeV. The COSY-11 result (closed circles) is compared to the data points determined at  $Q=15$  MeV by the TOF Collaboration (open circles) [21].

meson is identical with the direction of the movement of the proton-proton center-of-mass subsystem. The distribution of the differential cross section in  $\cos(\theta_{pp}^{**})$  is given in Table I of Ref. [32]. In this table we listed also the differential cross section as a function of angle  $\theta_{pp}^{**}$  of the relative proton momentum seen from the overall center-of-mass frame, as this is often considered in theoretical works. In Fig. 11 our results are compared to the angular distribution extracted by the TOF Collaboration. Both experiments agree very well within the statistical accuracy and indicate a slight decrease of the cross section with increasing  $|\cos(\theta_{pp}^{**})|$ .

#### IV. INTERPRETATION OF RESULTS

The interaction between particles depends on their relative momenta or equivalently on the invariant masses of the different combinations of the two-particle subsystems. Therefore modifications of the phase-space abundance should appear in the kinematical regions where the outgoing particles possess small relative velocities.

Figure 12 presents the projection of the phase-space distribution onto the square of the proton-proton invariant mass ( $s_{pp}$ ). The superimposed lines correspond to the calculations performed under the assumption that the production amplitude can be factorized into a primary production and final state interaction. The dotted lines result from calculations where only the proton-proton FSI was taken into account, whereas the thick-solid lines present results where the overall enhancement was factorized into the corresponding pair interactions of the  $pp\eta$  system. This factorization Ansatz is of course only valid if the different amplitudes are completely decoupled which is certainly not the case here. Therefore, these calculations should be considered as a rough estimate of the effect introduced by the FSI in the different two-body systems. The enhancement factor accounting for the proton-proton FSI has been calculated [14,37] as the square of the on-shell proton-proton scattering amplitude derived accord-

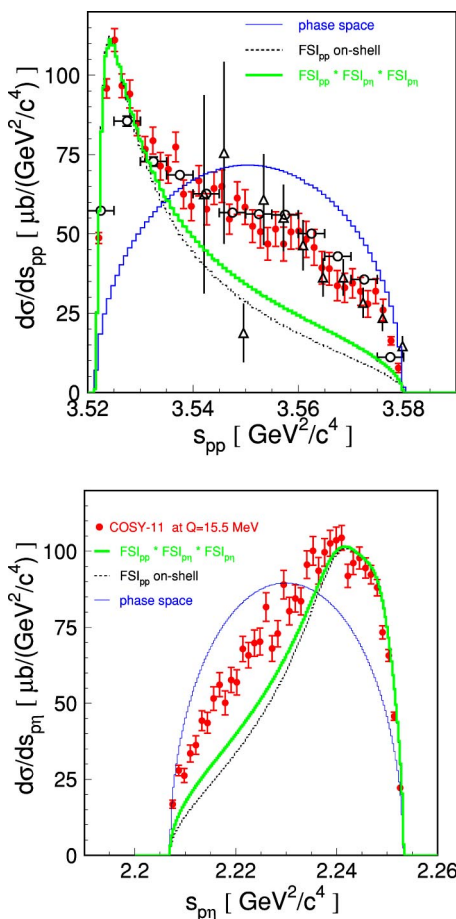


FIG. 12. Distributions of the squares of the proton-proton ( $s_{pp}$ ) and proton- $\eta$  ( $s_{p\eta}$ ) invariant masses determined experimentally for the  $pp \rightarrow pp\eta$  reaction at the excess energy of  $Q=15.5$  MeV by the COSY-11 Collaboration (closed circles), at  $Q=15$  MeV by the TOF Collaboration (open circles) [21], and at  $Q=16$  MeV by PROMICE/WASA (open triangles) [30]. The TOF and PROMICE/WASA data have been normalized to those of COSY-11, since these measurements did not evaluate the luminosities but rather normalized the results to Ref. [5] (see also comment [34]). The integrals of the phase-space weighted by the square of the proton-proton on-shell scattering amplitude (dotted lines)— $\text{FSI}_{pp}$ , and by the product of  $\text{FSI}_{pp}$  and the square of the proton- $\eta$  scattering amplitude (thick-solid lines) have been normalized arbitrarily at small values of  $s_{pp}$ . The thick-solid line was obtained assuming a scattering length of  $a_{p\eta}=0.7 \text{ fm} + i0.4 \text{ fm}$ . The expectation under the assumption of the homogeneously populated phase space are shown as thin-solid curves.

ing to the modified Cini-Fubini-Stanghellini formula including the Wong-Noyes Coulomb corrections [38]. The homogeneous phase-space distribution (thin-solid lines) deviates strongly from the experimentally determined spectra. The curves including the proton-proton and proton- $\eta$  FSI reflect the shape of the data for small invariant masses of the proton-proton system, yet they deviate significantly for large  $s_{pp}$  and small  $s_{p\eta}$  values. An explanation for this discrepancy could be a contribution from  $P$ -wave proton-proton interac-

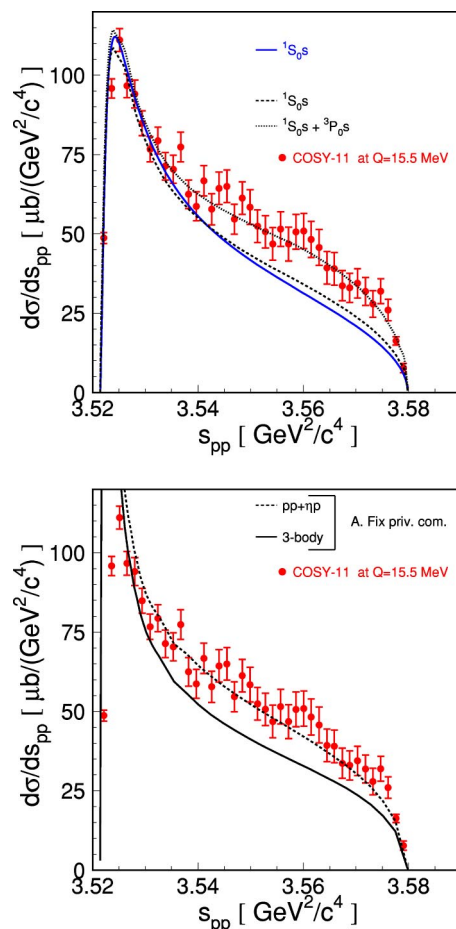


FIG. 13. (Upper picture) Distribution of the square of the proton-proton ( $s_{pp}$ ) invariant mass for the  $pp \rightarrow pp\eta$  reaction at an excess energy of  $Q=15.5$  MeV. Solid and dashed lines correspond to the calculations under the assumption of the  ${}^3P_0 \rightarrow {}^1S_0$  transition according to the models described in Refs. [10,39] and Refs. [11,40], respectively. The dotted curve shows the result with the inclusion of the  ${}^1S_0 \rightarrow {}^3P_0$  contribution as suggested in Ref. [11]. (Lower picture) The same data as above but with curves denoting preliminary three-body calculations [18] of the final  $pp\eta$  system as described in Ref. [41]. At present only the dominant transition  ${}^3P_0 \rightarrow {}^1S_0$  is taken into account and the production mechanism is reduced to the excitation of the  $S_{11}(1535)$  resonance via the exchange of the  $\pi$  and  $\eta$  mesons. The solid line was determined with the rigorous three-body approach [18] where the proton-proton sector is described in terms of the separable Paris potential (PEST3) [42], and for the  $\eta$ -nucleon scattering amplitude an isobar model analogous to the one of Ref. [43] is used with  $a_{\eta N}=0.5 \text{ fm} + i0.32 \text{ fm}$ . The dashed line is obtained if only pairwise interactions ( $pp+p\eta$ ) are allowed. The effect of proton-proton FSI at small  $s_{pp}$  is overestimated due to neglect of Coulomb repulsion between the protons. The lines are normalized arbitrarily but their relative amplitude is fixed from the model.

tion [11] or a possibly inadequate assumption that proton- $\eta$  and proton-proton interaction modify the phase-space occupations only as incoherent weights [36].

A slightly better description is achieved when the proton-proton interaction is accounted for by the realistic nucleon-

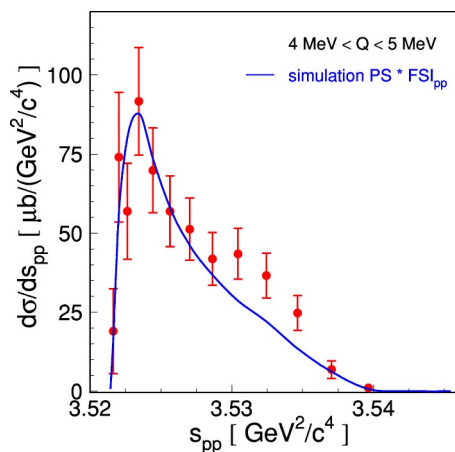


FIG. 14. Distribution of square of the proton-proton invariant mass from the  $pp \rightarrow pp\eta$  reaction measured at COSY-11 for the excess energy range  $4 \text{ MeV} \leq Q \leq 5 \text{ MeV}$  [6,44]. Numerical values are listed in Table III (see the electronic addendum to this paper [32]). The superimposed line shows the result of simulations performed under the assumption that the phase-space population is determined exclusively by the on-shell interaction between outgoing protons.

nucleon potential. The upper picture in Fig. 13 depicts the results obtained using two different models for the production process as well as for the  $NN$  interaction [10,39,11,40].

The calculations for the  ${}^3P_0 \rightarrow {}^1S_0s$  transition differ slightly, but the differences between the models are, by far, smaller than the observed signal.

Therefore we can safely claim that the discussed effect is rather too large to be caused by the particular assumptions used for the production operator and  $NN$  potential.

As can be seen in Fig. 9, the distribution of the  $\eta$  polar angle in the center-of-mass frame is fully isotropic. This is the next evidence — besides the shape of the excitation function and the kinematical arguments discussed in Ref. [14] — that at this excess energy ( $Q=15.5 \text{ MeV}$ ) the  $\eta$  meson is produced in the center-of-mass frame predominantly with the angular momentum equal to zero. Similarly, the distribution determined for the polar angle of the relative proton-proton momentum with respect to the momentum of the  $\eta$  meson as seen in the di-proton rest frame is also consistent with isotropy. Anyhow, even the isotropic distribution in this angle does not imply directly that the relative angular momentum between protons is equal to zero, because of their internal spin equal to  $\frac{1}{2}$ . Therefore, the contribution from the  ${}^3P_0$ -wave produced via the  ${}^1S_0 \rightarrow {}^3P_0s$  transition cannot be excluded. The isotropic angular distribution, as pointed out in Ref. [11], can also be principally achieved by the destructive interference between the transitions  ${}^1S_0 \rightarrow {}^3P_0s$  and  ${}^1D_2 \rightarrow {}^3P_2s$ .

As shown in Ref. [11] the invariant mass distributions can be very well described when including higher partial-wave amplitudes. In fact, as depicted by the dotted line in the upper panel of Fig. 13, an admixture of the  ${}^1S_0 \rightarrow {}^3P_0s$  transition leads to the excellent agreement with the experimen-

tally determined invariant mass spectra. However, at the same time, the model of Ref. [11] leads to strong discrepancies in the shape of the excitation function as can be deduced from the comparison of the dash-dotted line and the data in Fig. 1. Whereas it describes the data points in the excess energy range between 40 MeV and 100 MeV, it underestimates the total cross section below 20 MeV by a factor of 2.

Interestingly, the enhancement at large  $s_{pp}$  is visible also at much lower excess energy. This can be concluded from Fig. 14 in which the COSY-11 data at  $Q \approx 4.5 \text{ MeV}$  [44] are compared to the simulations based on the assumption that the phase-space abundance is due to the proton-proton FSI only. This observation could imply that the effect is caused by the proton- $\eta$  interaction rather than higher partial waves, since their contribution at such small energies is quite improbable [14]. However, as shown in the lower part of Fig. 13 the rigorous three-body treatment of the  $pp\eta$  system leads at large values of  $s_{pp}$  to the reduction of the cross section in comparison to the calculation taking into account only first-order rescattering ( $pp+p\eta$ ) [18]. Here, both calculations include only the  ${}^3P_0 \rightarrow {}^1S_0s$  transition. Though the presented curves are still preliminary, we can qualitatively assess that the rigorous three-body approach, in comparison to the present estimations, will on one hand enhance the total cross section near threshold as shown in Fig. 1, while on the other hand it will decrease the differential cross section at large values of  $s_{pp}$ . This is just opposite to the influence of  $P$  waves in the proton-proton system.

From the above presented considerations it is rather obvious that the rigorous three-body treatment of the produced  $pp\eta$  system and the exact determination of the contributions from the higher partial waves may result in the simultaneous explanation of both observations: the near-threshold enhancement of the excitation function of the total cross section and the strong increase of the invariant mass distribution at large values of  $s_{pp}$ . For the unambiguous determination of the contributions from different partial waves spin dependent observables are required [11]. The first attempt has been already reported in Ref. [45].

## V. CONCLUSION

Using the stochastically cooled proton beam at the Cooler Synchrotron COSY and the COSY-11 facility we have determined the total and differential cross sections for the  $pp \rightarrow pp\eta$  reaction at an excess energy of  $Q=15.5 \text{ MeV}$ . The high statistics data sample allowed for the clear separation of events corresponding to the  $pp \rightarrow pp\eta$  reaction from the multiplication production at each investigated phase-space bin, and the multidimensional acceptance correction allowed to extract the result without the necessity of any assumption about the reaction process.

The determined distributions of the center-of-mass polar angle of the  $\eta$  meson emission as well as the distribution of the relative proton-proton momentum with respect to the momentum of the  $\eta$  meson are consistent with isotropy, though in the latter a small tendency of an increase of the cross section at  $90^\circ$  is observed. In contrast a rather strong decrease of the cross section was found at  $90^\circ$  for the center-

of-mass polar angle of the vector normal to the emission plane. Explanation of that effect may reveal an interesting characteristic of the dynamics of the production process.

The determined invariant mass spectra of the two-particle subsystems deviate strongly from the predictions based on the homogeneous population of events over the phase space. Deviations at low proton-proton invariant mass values can be well explained as an influence of the  $S$ -wave interaction between the two protons. However, an unexpectedly large enhancement of the occupation density in the kinematical regions of low  $\eta$ -proton relative momentum is not yet understood. We have demonstrated that for the simultaneous description of the excitation function and invariant mass dis-

tributions a rigorous three-body calculation with inclusion of the contribution from higher partial waves is needed.

#### ACKNOWLEDGMENTS

We thank the stimulating discussions and help of V. Baru, A. Fix, and Ch. Hanhart. The work was partly supported by the European Community-Access to Research Infrastructure action of the Improving Human Potential Programme as well as the Internationales Büro and the Verbundforschung of the BMBF, and by the Polish State Committee for Scientific Research (Grant No. 2P03B07123).

- 
- [1] F. Balestra *et al.*, Phys. Lett. B **491**, 29 (2000); R. Wurzinger *et al.*, *ibid.* **374**, 283 (1996); P. Moskal *et al.*, *ibid.* **474**, 416 (2000); P. Moskal *et al.*, Phys. Rev. Lett. **80**, 3202 (1998); A. Khoukaz *et al.*, IKP Universität Annual Report, 2001 (unpublished).
- [2] F. Hibou *et al.*, Phys. Lett. B **438**, 41 (1998).
- [3] E. Chiavassa *et al.*, Phys. Lett. B **322**, 270 (1994); H. Calén *et al.*, Phys. Rev. Lett. **79**, 2642 (1997).
- [4] A. M. Bergdolt *et al.*, Phys. Rev. D **48**, R2969 (1993).
- [5] H. Calén *et al.*, Phys. Lett. B **366**, 39 (1996).
- [6] J. Smyrski *et al.*, Phys. Lett. B **474**, 182 (2000).
- [7] H. O. Meyer *et al.*, Nucl. Phys. **A539**, 633 (1992); A. Bondar *et al.*, Phys. Lett. B **356**, 8 (1995); J. Greiff *et al.*, Phys. Rev. C **62**, 064002 (2000); M. Betigeri *et al.*, Nucl. Phys. **A690**, 473 (2001); D. A. Hutcheon *et al.*, Phys. Rev. Lett. **64**, 176 (1990).
- [8] H. O. Meyer *et al.*, Phys. Rev. C **63**, 064002 (2001).
- [9] M. Batinić *et al.*, Phys. Scr. **56**, 321 (1997); A. Moalem *et al.*, Nucl. Phys. **A600**, 445 (1996); J. F. Germond and C. Wilkin, *ibid.* **A518**, 308 (1990); J. M. Laget *et al.*, Phys. Lett. B **257**, 254 (1991); T. Vetter *et al.*, *ibid.* **263**, 153 (1991); B. L. Alvarez and E. Oset, *ibid.* **324**, 125 (1994); M. T. Peña *et al.*, Nucl. Phys. **A683**, 322 (2001); F. Kleefeld and M. Dillig, Acta Phys. Pol. B **29**, 3059 (1998); S. Ceci and A. Švarc, nucl-th/0301036.
- [10] V. Baru *et al.*, Phys. Rev. C **67**, 024002 (2003).
- [11] K. Nakayama *et al.*, nucl-th/0302061.
- [12] K. Nakayama *et al.*, Phys. Rev. C **61**, 024001 (1999); E. Gedalin *et al.*, Nucl. Phys. **A650**, 471 (1999); V. Baru *et al.*, Eur. Phys. J. A **6**, 445 (1999); S. Bass, Phys. Lett. B **463**, 286 (1999); A. Sibirtsev and W. Cassing, Eur. Phys. J. A **2**, 333 (1998).
- [13] V. Bernard, N. Kaiser, and Ulf-G. Meißner, Eur. Phys. J. A **4**, 259 (1999).
- [14] P. Moskal, M. Wolke, A. Khoukaz, and W. Oelert, Prog. Part. Nucl. Phys. **49**, 1 (2002).
- [15] G. Fäldt, T. Johansson, and C. Wilkin, Phys. Scr. **T99**, 146 (2002).
- [16] H. Machner *et al.*, J. Phys. G **25**, R231 (1999).
- [17] A. M. Green and S. Wycech, Phys. Rev. C **55**, R2167 (1997).
- [18] A. Fix and H. Arenhövel (unpublished).
- [19] V. Hejny *et al.*, Eur. Phys. J. A **13**, 493 (2002); Ch. Elster *et al.*, nucl-th/0207052; A. Sibirtsev *et al.*, Phys. Rev. C **65**, 067002 (2002).
- [20] U. Schuberth, Ph.D. thesis, University of Uppsala, Acta Universitatis, Upsaliensis, 1995.
- [21] M. Abdel-Bary *et al.*, Eur. Phys. J. A **16**, 127 (2003).
- [22] E. Roderburg *et al.*, Acta Phys. Pol. B **31**, 2299 (2000).
- [23] S. Brauksiepe *et al.*, Nucl. Instrum. Methods Phys. Res. A **376**, 397 (1996).
- [24] P. Moskal *et al.*, Nucl. Instrum. Methods Phys. Res. A **466**, 448 (2001).
- [25] D. Prasuhn *et al.*, Nucl. Instrum. Methods Phys. Res. A **441**, 167 (2000).
- [26] H. Dombrowski *et al.*, Nucl. Instrum. Methods Phys. Res. A **386**, 228 (1997).
- [27] P. Moskal, Ph.D. thesis, Jagellonian University, Cracow, 1998.
- [28] Particle Data Group, K. Hagiwara *et al.*, Phys. Rev. D **66**, 010001 (2002).
- [29] J. Ritman, Habilitation thesis, Gießen University, 2000.
- [30] H. Calén *et al.*, Phys. Lett. B **458**, 190 (1999).
- [31] F. Balestra *et al.*, Phys. Rev. Lett. **89**, 092001 (2002).
- [32] See EPAPS Document No. E-PRVCAN-68-015312 for the electronic addendum to this paper. It comprises Tables I, II and III. A direct link to this document may be found in the online article's homepage (<http://www.aip.org/pubservs/epaps.html>) or from <ftp.aip.org> in the directory /epaps/. See the EPAPS homepage for more information.
- [33] D. Albers *et al.*, Phys. Rev. Lett. **78**, 1652 (1997).
- [34] The WASA/PROMICE Collaboration determined the total cross section of  $2.11 \pm 0.74$  (overall error) at  $Q = 15.0 \pm 0.5$  MeV [5]. This value is by about 30% lower than our result, though the values still agree with each other if one adds the statistical and systematical uncertainties. However, the acceptance correction for this experiment was calculated taking into account the phase-space distribution only [20] and this leads to the underestimation of the total cross section which can be deduced from the comparison between the  $s_{pp}$  distribution and the phase-space prediction shown in Fig. 12. For the discussion of that issue see also Ref. [46]. Our result agrees, however, quite well with the value of  $2.68 \pm 0.54 \mu\text{b}$  determined at  $Q = 16 \pm 0.6$  MeV [4] at the SATURNE facility [2].
- [35] D. Grzonka and K. Kilian, in Proceedings of the Symposia on

- Threshold Meson Production in  $pp$  and  $pd$  Interactions, Cracow, Poland, 2001, edited by P. Moskal and M. Wolke, Schriften des FZ-Jülich Matter & Materials Vol. 11, 2002, p. 100.
- [36] For the discussion of the FSI effects see, e.g., F. Kleefeld, nucl-th/0108064; in Proceedings of the Symposia on Threshold Meson Production in  $pp$  and  $pd$  Interactions, Cracow, Poland, 2001 (Ref. [35]), p. 51.
- [37] P. Moskal *et al.*, Phys. Lett. B **482**, 356 (2000).
- [38] H. P. Noyes and H. M. Lipinski, Phys. Rev. C **4**, 995 (1971).
- [39] V. Baru (private communication).
- [40] Here the model described in Ref. [11] was improved and the Coulomb interaction between protons was taken into account.
- [41] A. Fix and H. Arenhövel, Nucl. Phys. **A697**, 277 (2002).
- [42] J. Haidenbauer and W. Plessas, Phys. Rev. C **30**, 1822 (1984).
- [43] C. Bennhold and H. Tanabe, Nucl. Phys. **A530**, 625 (1991).
- [44] J. Smyrski *et al.*, IKP FZ-Jülich Annual Report Jül-3640 39, 1999 (unpublished).
- [45] P. Winter *et al.*, Phys. Lett. B **544**, 251 (2002); **553**, 339(E) (2003).
- [46] S. AbdEl Samad *et al.*, Eur. Phys. J. A **17**, 595 (2003).